emesent

M300/M350 RTK: IMPROVED SLAM ACCURACY AND GEOREFERENCING WHITE PAPER

DOCUMENT NUMBER: INF-001
REVISION NUMBER: 1.1
RELEASE DATE: 01 MAR 2024

PREPARED BY:
EMESENT PTY LTD
LEVEL 6, BUILDING 4, KINGS ROW OFFICE PARK
40-52 MCDOUGALL ST, MILTON, QLD, 4064 AUSTRALIA

EMAIL: CUSTOMER-SUCCESS@EMESENT.IO
PHONE: +61 7 3548 9494

Copyright

The content of this document is confidential and intended for reading only by the addressee. All rights including Intellectual Property Rights flowing from, incidental to or contained in this document irrevocably vest in Emesent unless otherwise agreed to in writing.

©Emesent 2024

Using this manual

Hovermap is a powerful system that can be used as a Lidar mapping payload but also as an advanced autopilot for drones. It is therefore recommended to read the user manual thoroughly to make use of all its capabilities in a safe and productive way.

Disclaimer and safety guidelines

This product is not a toy and must not be used by any person under the age of 18. It must be operated with caution, common sense, and in accordance with the instructions in the user manual. Failure to operate it in a safe and responsible manner could result in product loss or injury.

By using this product, you hereby agree that you are solely responsible for your own conduct while using it, and for any consequences thereof. You also agree to use this product only for purposes that are in accordance with all applicable laws, rules and regulations.

The use of Remotely Piloted Aircraft Systems (RPAS) may result in serious injury, death, or property damage if operated without proper training and due care. Before using an RPAS, you must ensure that you are suitably qualified, have received all necessary training, and read all relevant instructions, including the user manual. When using an RPAS, you must adopt safe practices and procedures at all times.

Warnings

- This document is legally privileged, confidential under applicable law and is intended only for the use of the individual or entity to whom it is addressed. If you have received this transmission in error, you are hereby notified that any use, dissemination, distribution or reproduction is strictly prohibited. If you are not the intended recipient, please notify the sender and delete the message from your system.

- Always be aware of moving objects that may cause serious injury, such as spinning propellers or other components. *Never* approach a drone while the propellers are spinning or attempt to catch an airborne drone.

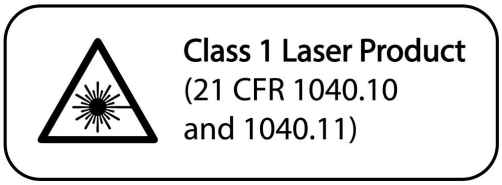

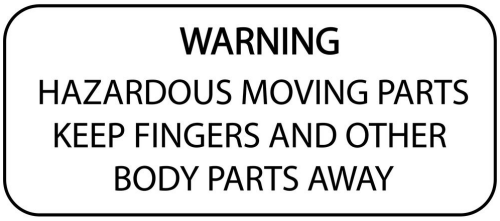

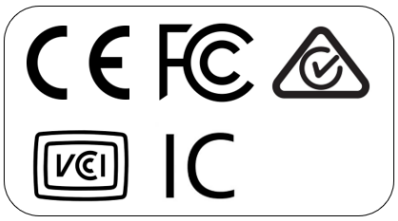

Contents

1. Introduction

GPS receiver data in general, and Real-Time Kinematic (RTK) GPS data in particular, are auxiliary sources of information that can be utilized to correct SLAM (Simultaneous Localization and Mapping) drift and also geo-reference LiDAR point clouds. These processes are analogous to using Ground Control Points (GCPs) in the Emesent Aura software, where data is aligned to the corresponding survey coordinates of targets.

Utilizing the RTK capability can improve SLAM performance in low-feature areas and/or long-duration scans as well as georeferencing the point cloud. It also can enable Hovermap to perform drift correction without needing to “close the loop” as well as perform a dense scan of the environment.

1.1 Processing Workflow

RTK processing requires a connection between the drone and a base station during data capture with Hovermap automatically recording the timestamped positions of the drone along with LiDAR data in the BAG files. The BAG files are then managed in a processing pipeline transparent to the end user as summarized in **Figure 1**.

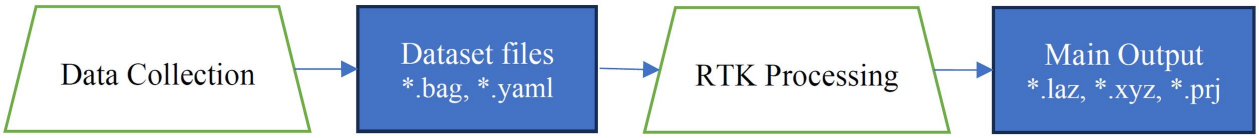

Figure 1 General data processing pipeline

The output consists of a PRJ file describing how the point cloud coordinate reference can be connected to other coordinate systems. It defines a local Transverse Mercator coordinate system at the center of the point cloud coordinate system to mitigate the scaling risk of point coordinates as they get farther from the center of the coordinate system.

2. Understanding RTK Data

RTK data is used to improve SLAM by adding information about the position of Hovermap. This information serves as auxiliary constraints letting SLAM know about the global location of Hovermap at different times. As a result, SLAM drift is corrected even without the need for loop closure and also the resultant point cloud is geo-referenced.

SLAM processing using RTK consists of three main steps:

- RTK data filtering
- fitting SLAM to RTK data
- georeferenced output generation.

These are discussed in detail in the succeeding sections.

2.1 RTK Data Filtering

RTK data can have inherent uncertainty, depending on the visible satellite constellation at the base, rover, and also the real-time link between the base station and the drone.

SLAM can compensate for the uncertainty in RTK data to some extent. However, providing highly uncertain observations can lead to poor results and misinform the SLAM process. Similarly, over-constraining SLAM with too many uncertain limitations could also negatively impact the quality of the SLAM. Therefore, applying proper outlier rejection and filtering on recorded RTK coordinates is crucial for a robust projection of the point cloud.

Emesent Aura's Outlier Rejection algorithms can remove low-confidence RTK samples, and the GPS Subsampler can reduce both the temporal and spatial frequency of valid RTK samples.

Table 1 Basic Filtering policies in place

Policy	Purpose	Description
Outlier Rejection	Filtering	For removing unreliable RTK samples and also to avoid misleading SLAM
GPS Subsampler	Filtering	For reducing RTK sampling frequency and also to avoid SLAM over constraining

2.2 Fitting SLAM to RTK Data

Once valid RTK data is extracted, it is incorporated into the SLAM process to limit the position of the Hovermap at different times. These observations are then used to correct the SLAM trajectory to the RTK trajectory. However, it's important to note that the resulting corrected trajectory may not exactly match the RTK trajectory due to some uncertainty within the RTK correction.

Figure 2 illustrates how RTK observations aid SLAM in improving the trajectory. At the right end of the original Hovermap trajectory, SLAM drifts, but this is adjusted to match the given RTK coordinates. As a result, the final SLAM-corrected RTK trajectory is produced as a dotted blue line. The grey arrows indicate *Observation Pose* which is the disparity between the output trajectory and the RTK antenna of the drone.

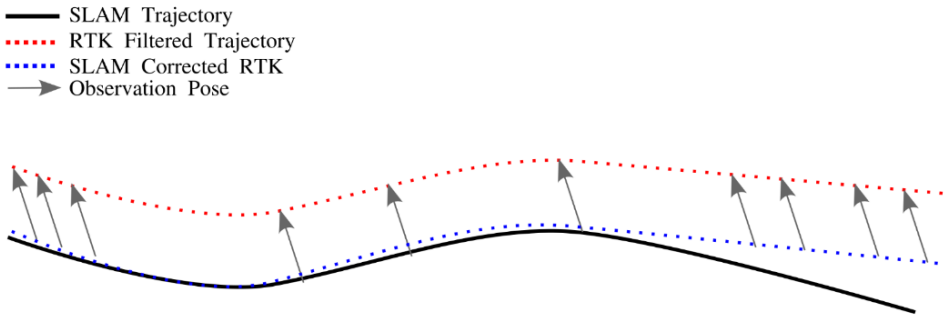

Figure 2 Example trajectory correction (black line) using recorded pose observations (gray arrows) resulting in the final SLAM-corrected RTK trajectory (dotted blue line)

2.3 Georeferenced Output Generation

Once the SLAM trajectory has been corrected using the RTK trajectory, the next step is to georeference the trajectory by projecting the trajectory and associated mapping data into a desired Coordinate Reference System (CRS). Emesent Aura automatically generates the CRS in a PRJ file which can be used by the GIS software for importing resultant data.

The outcome of the georeferencing process is an implicitly georeferenced point cloud. This means that instead of georeferencing each point, their reference point (i.e. position of the LiDAR sensor) is adjusted, and as a result, the points in the point cloud are positioned in their corresponding georeferenced locations.

3. M300 RTK Accuracy Analysis

A set of experiments has been conducted to assess the robustness and correctness of georeferenced point clouds in various data collection scenarios by collecting data at different flight speeds, various flight trajectories, longer flight times, and larger mapping areas.

3.1 Experiment Setup

The trials were conducted in an environment where ground-truth data was available, allowing for the accuracy of the RTK solution to be measured. An open field with GCP targets was selected to stress-test the RTK approach in a relatively featureless environment (i.e. few geometric features that SLAM requires for locating position and tracking movement). Twenty 60cm (in diameter) Emesent GCP targets were positioned and surveyed in the field. The arrangement of the GCP targets in the field is illustrated in **Figure 3**.

Figure 3 Aerial imagery illustrating the position and layout of Ground Control Point (GCP) targets (white circles, not to scale) utilized in this study

For each trial, a DJI M300 drone equipped with a Hovermap ST-X was used. The experiments were divided into two categories, both of which were conducted at an altitude of 30 meters. In the first category, the drone flew at a speed of 3 m/s, while in the second category, it flew at a speed of 6 m/s.

To account for differences among various Hovermap and drone configurations, each experiment was executed twice, using a different DJI M300 drone each time. This resulted in a total of four experiments.

Each GCP target was surveyed using an Emlid RS2 RTK GNSS receiver as a 'rover' GPS with a second Emlid RS2 unit deployed in the field to act as the base station connected to the Geoscience Australia Continuously Operating Reference Station (CORS) network (NTRIP protocol through the 4G network). This setup makes the center of the targets surveyed independent from global position accuracy and therefore based on a local coordinate system (i.e. accurate relative to each other).

The latitude, longitude, and ellipsoidal height of each GCP target were measured three times and averaged.

3.2 Accuracy Assessment Process

To assess RTK accuracy, the PRJ file is first applied to the surveyed coordinates of the GCP targets to transform them into the same frame as the point cloud. Next, the coordinates of the GCP targets in the point cloud are computed using Emesent's GCP target detection algorithm. Lastly, the error is computed as horizontal (xy_err), vertical (z_err), and 3D (xyz_err) distances between projected survey points and their corresponding target centers.

3.3 M300 RTK Accuracy Results

GCPs are surveyed by Emlid RS2 RTK GNSS with reported 10 mm Rooted Mean Square (RMS) error for Easting, Northing, and Elevation.

For each detected GCP target in the point cloud, absolute distances along all axes are computed and results are summarized in **Table 2** along with error distribution percentiles at 50%, 75%, and 90%. The first row in the table shows that there are 46 error measurement observations obtained from two different experiments (3m/s and 6m/s) each repeated by two different drones (4 flights in total).

We can determine the accuracy of georeferencing by looking at different error distribution percentiles such as 50%, 75%, and 90%. In this case, we used the 90% percentile to measure georeferencing confidence and to determine the expected accuracy of the RTK processing software. This means that in 90% of the observations, the absolute georeferencing error is less than or equal to 50mm in both horizontal and vertical directions. The 3D error at the 90% percentile is 56mm.

Table 2 Statistical descriptions of error distributions resulting from M300 trials

	x_err (m)	y_err (m)	xy_err(m)	z_err(m)	xyz_err(m)
No. Observation	46	46	46	46	46
Mean	0.0110	0.0147	0.0206	0.0385	0.0451
Std. Dev.	0.0089	0.0129	0.0126	0.0065	0.0083
Min	0.0000	0.0005	0.0014	0.0266	0.0319
50%	0.0098	0.0115	**0.0180**	**0.0387**	**0.0427**
75%	0.0168	0.0209	0.0253	0.0435	0.0489
90%	0.0241	0.0264	**0.0378**	**0.0466**	**0.0565**
Max	0.0306	0.0593	0.0624	0.0531	0.0712

Histogram plots of distribution errors are shown in **Figure 4.** It can be seen that distribution functions almost have a Gaussian shape. The median of each error function is illustrated by a vertical line and placed at 18mm, 38mm, and 42mm for horizontal, vertical, and 3D errors, respectively.

In summary, the accuracy of the system with one standard deviation falls at 20mm±12mm for horizontal accuracy, 38mm±6mm for vertical accuracy, and 45mm±8mm for 3D accuracy.

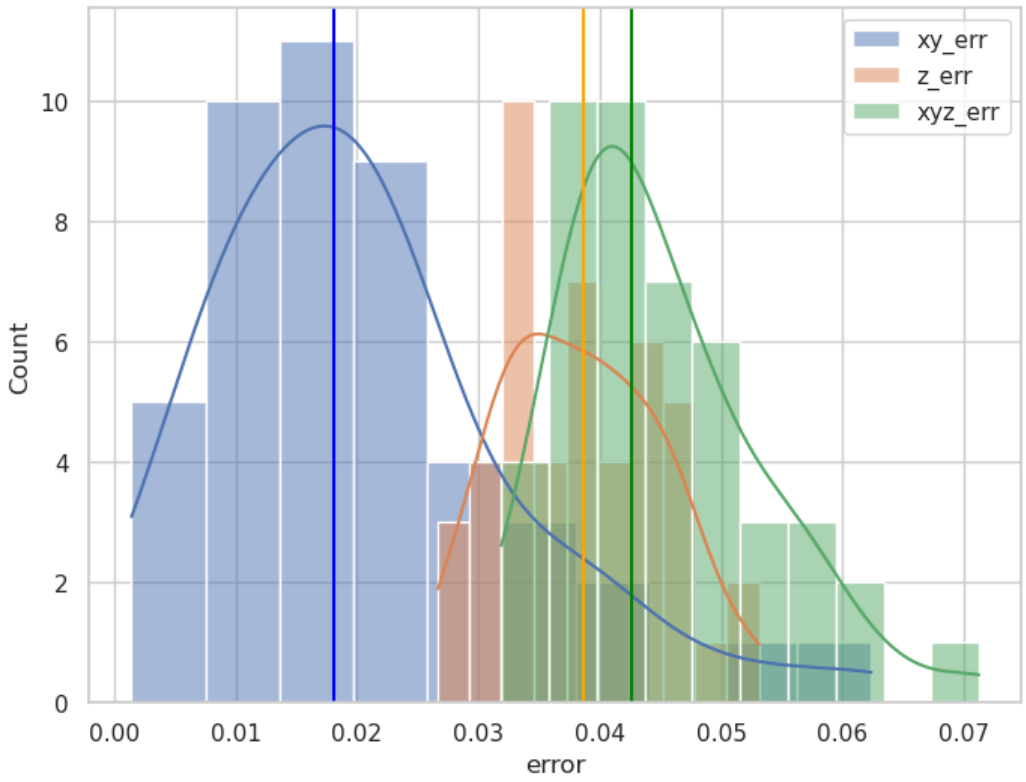

Figure 4 Distribution of horizontal (blue), vertical (orange), and 3D (green) georeferencing errors observed across the 46 accuracy evaluations. Vertical lines represent median error.

3.4 Accuracy Results at Different Velocities

This section provides an analysis of the error distribution for experiments collected at two different drone velocities (3 m/s and 6 m/s), both at 30m altitude. Each deployment was performed twice, each time with a different drone to evaluate potential differences between platforms.

The results are summarized in **Table 3**, which shows that at 90% percentile, both experiments are accurate to 50mm.

Table 3 Statistical descriptions of observed errors at 3 m/s and 6 m/s velocities

3 m/s - 30 m	x_err (m)	y_err (m)	xy_err(m)	z_err(m)	xyz_err(m)
Count	23	23	23	23	23
Mean	0.0133	0.0172	0.0245	0.0381	0.0469
Std. Dev.	0.0103	0.0160	0.0151	0.0051	0.0100
Min	0.0005	0.0005	0.0041	0.0292	0.0319
25%	0.0027	0.0055	0.0150	0.0339	0.0391
50%	0.0132	0.0144	**0.0195**	**0.0388**	**0.0450**
75%	0.0189	0.0216	0.0369	0.0413	0.0546
90%	0.0290	0.0386	**0.0424**	**0.0449**	**0.0592**
Max	0.0306	0.0593	0.0624	0.0480	0.0712

6 m/s - 30 m	x_err (m)	y_err (m)	xy_err(m)	z_err(m)	xyz_err(m)
Count	23	23	23	23	23
Mean	0.0088	0.0122	0.0166	0.0388	0.0432

6 m/s - 30 m	x_err (m)	y_err (m)	xy_err(m)	z_err(m)	xyz_err(m)
Std. Dev.	0.0068	0.0083	0.0078	0.0078	0.0057
Min	0.0000	0.0013	0.0014	0.0266	0.0342
25%	0.0033	0.0061	0.0097	0.0329	0.0393
50%	0.0093	0.0114	**0.0171**	**0.0387**	**0.0423**
75%	0.0130	0.0201	0.0240	0.0447	0.0475
90%	0.0170	0.0233	**0.0260**	**0.0476**	**0.0501**
Max	0.0244	0.0269	0.0286	0.0531	0.0561

The distribution of errors is shown in **Figure 5**. The violin plot illustrates the horizontal (XY) and vertical (Z) errors observed at ~20mm and ~38mm, respectively.

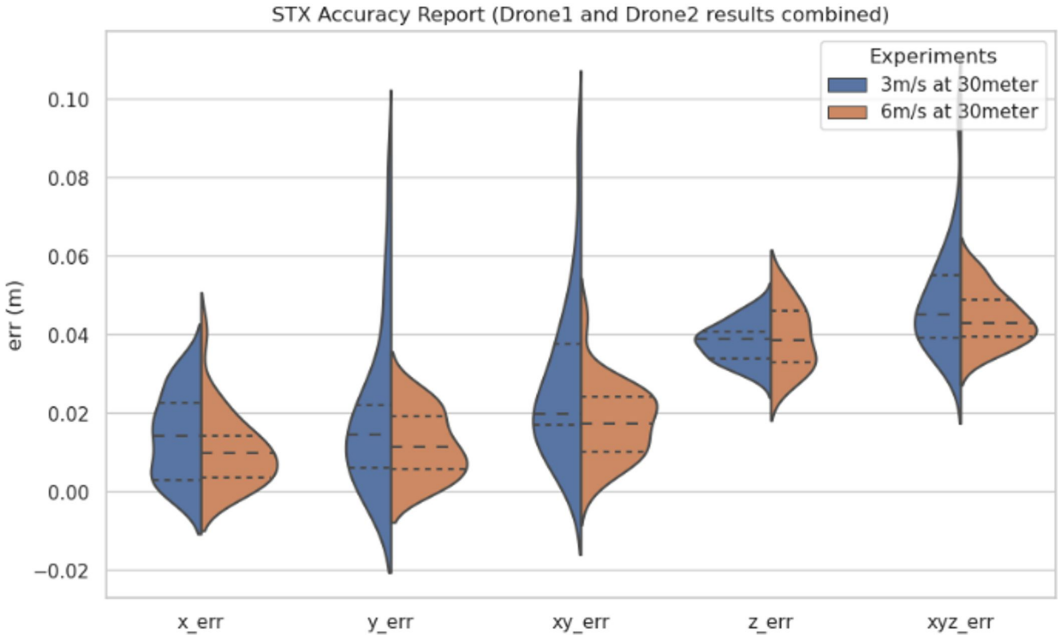

Figure 5 Observed horizontal and vertical errors across the drone flights at 3 m/s (blue) and 6 m/s (orange). Dashed lines correspond to 25%, 50%, and 75% percentiles.

4. M350 RTK Accuracy Analysis

Similar experiments have been conducted to assess the M350 RTK accuracy in the same environment as described below.

4.1 Experiment Setup

To capture drone and payload variability, two Hovermap ST-X payloads and two M350 drones were used for running the experiments. Also, two different flight paths, called *long-edge* and *mower path* (as illustrated in **Figure 6**) are designed for capturing mapping accuracy on different flight trajectories. These flight paths are designed to capture how flight path self-intersections and overlaps on RTK observation can affect accuracies. All experiments are performed at 30m altitude and 6m/s velocity.

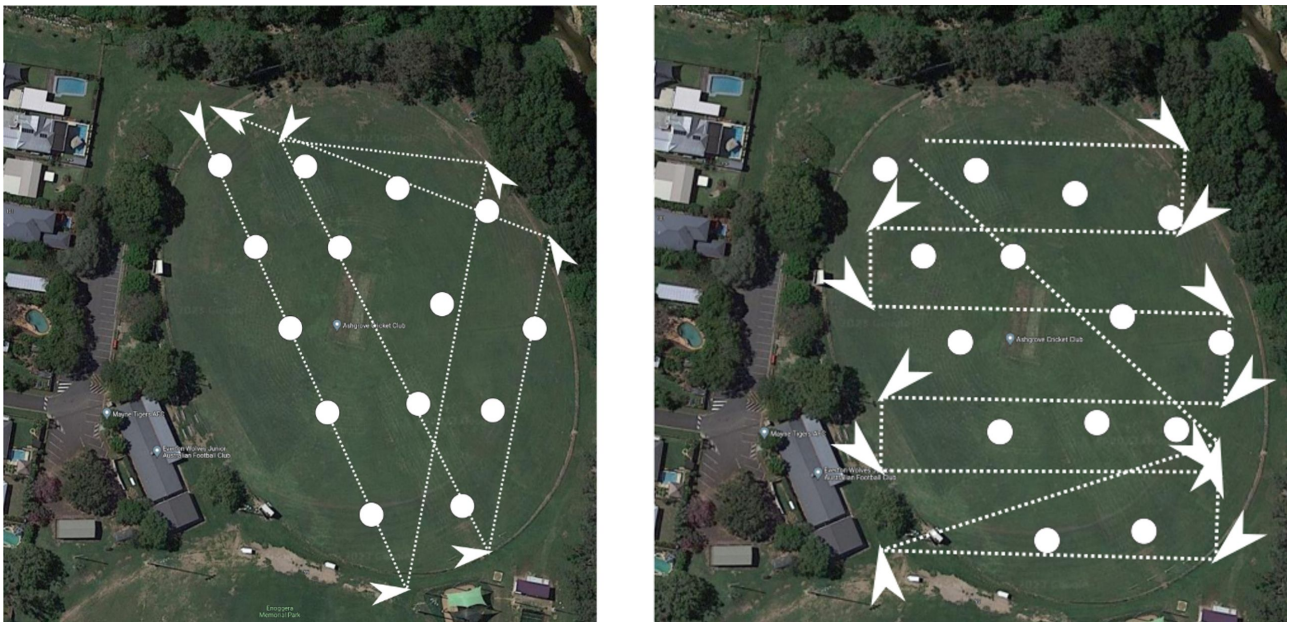

Figure 6 Flight trajectories used for M350 accuracy evaluations: (left) long-edge (right) mower path

4.2 M350 RTK Accuracy Results

A total of 16 different experiments were conducted and projection accuracy was evaluated for all detected GCP targets across all experiments, as summarized in **Table 4**. The first row of the table shows that there are 368 error measurement observations with a mean 3D error of 30.5mm and a standard deviation of 14.8mm.

We can determine the accuracy of georeferencing by looking at different error distribution percentiles such as 50%, 75%, and 90%. In this case, we used the 90% percentile to measure georeferencing confidence and to determine the expected accuracy of the RTK processing software. This means that in 90% of the observations, the absolute georeferencing error is less than or equal to 50mm in both horizontal and vertical directions. The 3D error at the 90% percentile is 51.7mm.

Table 4 Statistical descriptions of error distributions resulting from M300 trials

	x_err (m)	y_err (m)	xy_err(m)	z_err(m)	xyz_err(m)
No. Observation	368	368	368	368	368
Mean	0.0132	0.0106	0.0185	0.0220	**0.0305**
Std. Dev.	0.0091	0.0078	0.0094	0.0153	**0.0148**
Min	0.0000	0.0005	0.0013	0.0001	0.0045
50%	0.0111	0.0091	**0.0183**	**0.0202**	**0.0282**
75%	0.0195	0.0158	0.0249	0.0311	0.0396
90%	0.0267	0.0220	**0.0311**	**0.0431**	**0.0517**
Max	0.0419	0.0363	0.0481	0.0744	0.0777

Histogram plots of distribution errors are shown in **Figure 7**. It can be seen that distribution functions almost have a Gaussian shape. The median of each error function is illustrated by a vertical line and placed at 18mm, 20mm, and 28mm for horizontal, vertical, and 3D errors, respectively.

In summary, the accuracy of the system for M350 with one standard deviation falls at 18mm±9mm for horizontal accuracy, 22mm±15mm for vertical accuracy, and 30mm±15mm for 3D accuracy.

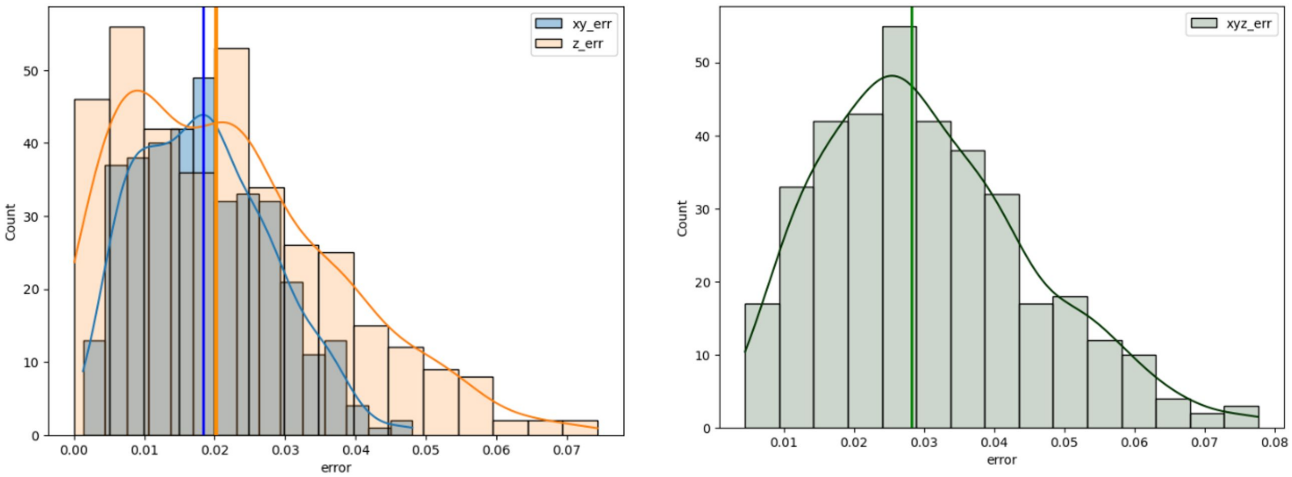

Figure 7 Distribution of horizontal (blue), vertical (orange), and 3D (green) georeferencing errors observed across the 368 accuracy evaluations for M350 RTK. Vertical lines represent median error.

4.3 Comparing the Accuracy of Flight Paths

To determine whether or not flight trajectory affects accuracy, the error distribution was computed for each flight path type as illustrated in **Figure 8**. The findings suggest that there is no significant difference in accuracy between long-edge and mower path flight trajectories. However, self-intersections can reinforce the production of robust georeferenced point clouds. Refer to the following section for more detailed information.

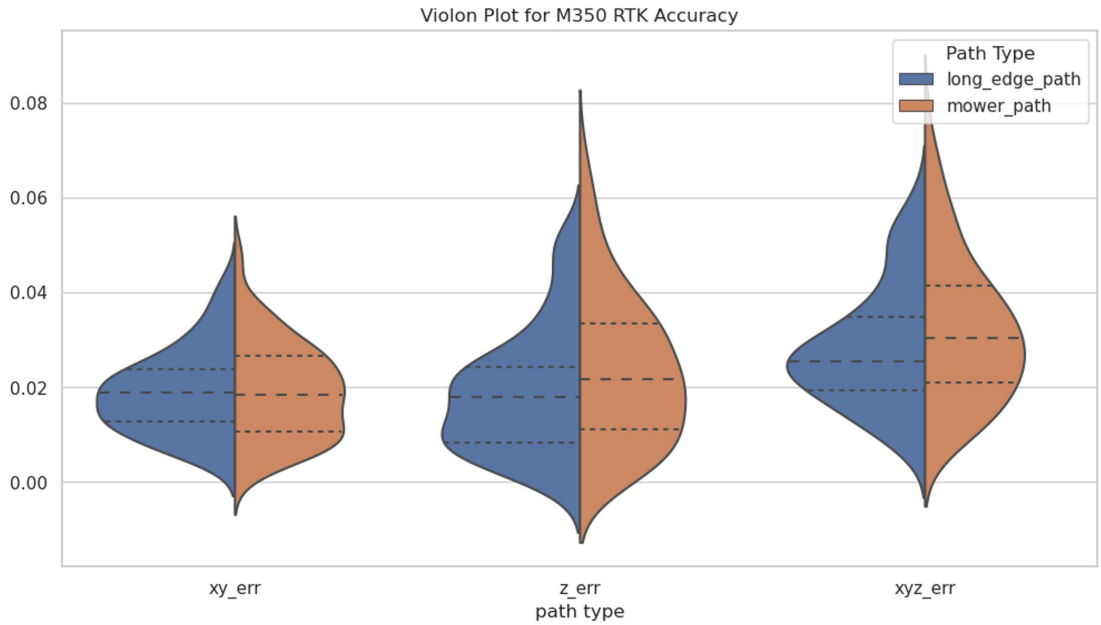

Figure 8 Error distribution for long edge vs mower path types

5. Implicit Georeferencing

The accuracy assessments mentioned above were evaluated in relation to the surveyed GCP target coordinates and provided a discrete evaluation of georeferencing errors. To convert these evaluations into a continuous domain, the Radial Basis Function (RBF) interpolation technique is used. **Figure 9** illustrates the "heat map" result of the RBF interpolation for horizontal (XY) accuracy, where the red line represents the flight trajectory, and the annotated points are associated with the survey points.

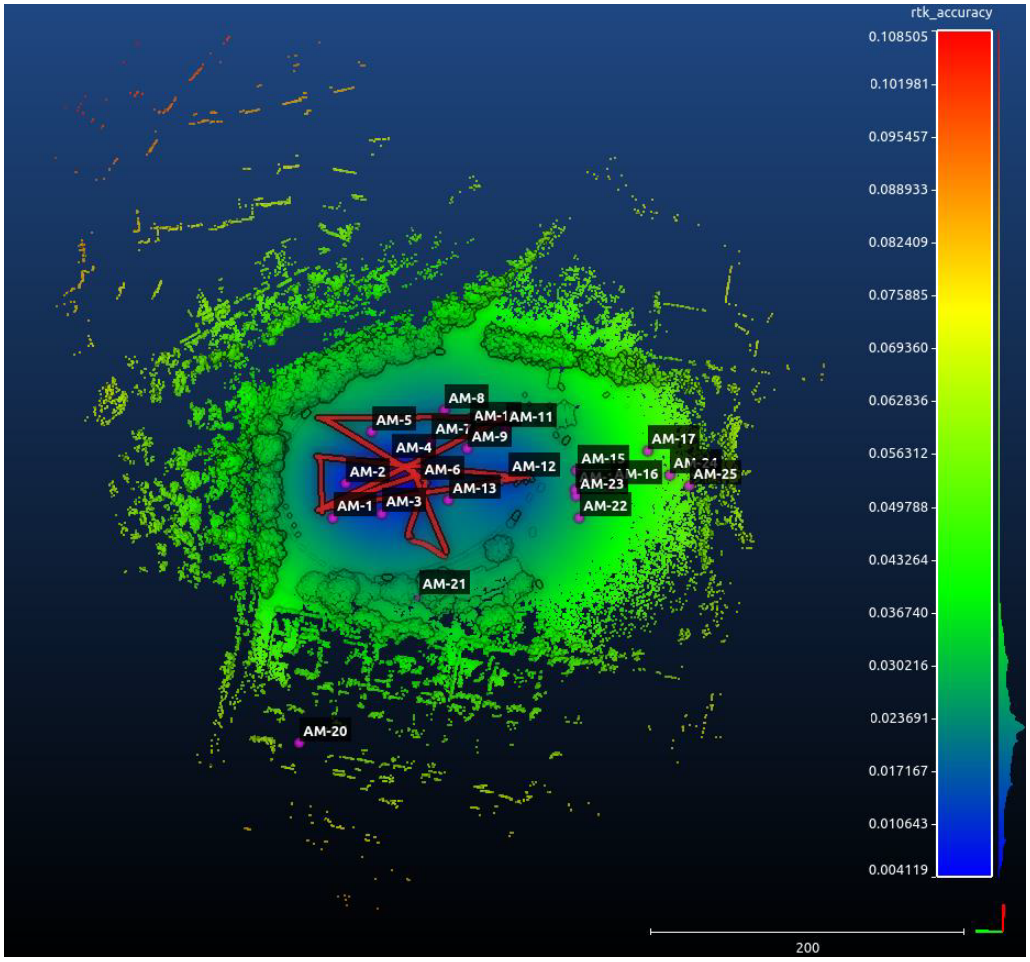

Figure 9 Flight trajectory is displayed as a red line, with a heat map representing horizontal error, where blue indicates lower error and red indicates higher error.

The heat map's color gradient indicates the accuracy of data points. Blue represents highly accurate areas with errors as low as 4mm, while green represents medium accuracy within the 20mm to 50mm range. Towards the point cloud's outer edges, beyond a 130m radius from the trajectory, you may observe data points in the yellow to red spectrum, which correspond to lower accuracy ranging from 70mm to 100mm. However, the occurrence of such points is minimal and constitutes only a tiny fraction of the entire point cloud.

Figure 10 displays the histogram of the RBF approximation of errors. The distribution reveals that the RBF error adheres to a Gaussian distribution with a mean of 22mm and a standard deviation of 8mm. Notably, the vertical red line serves as a reference, indicating that the majority (99.43%) of points fall within the blue to green range of the heat map colors, corresponding to errors less than 50mm.

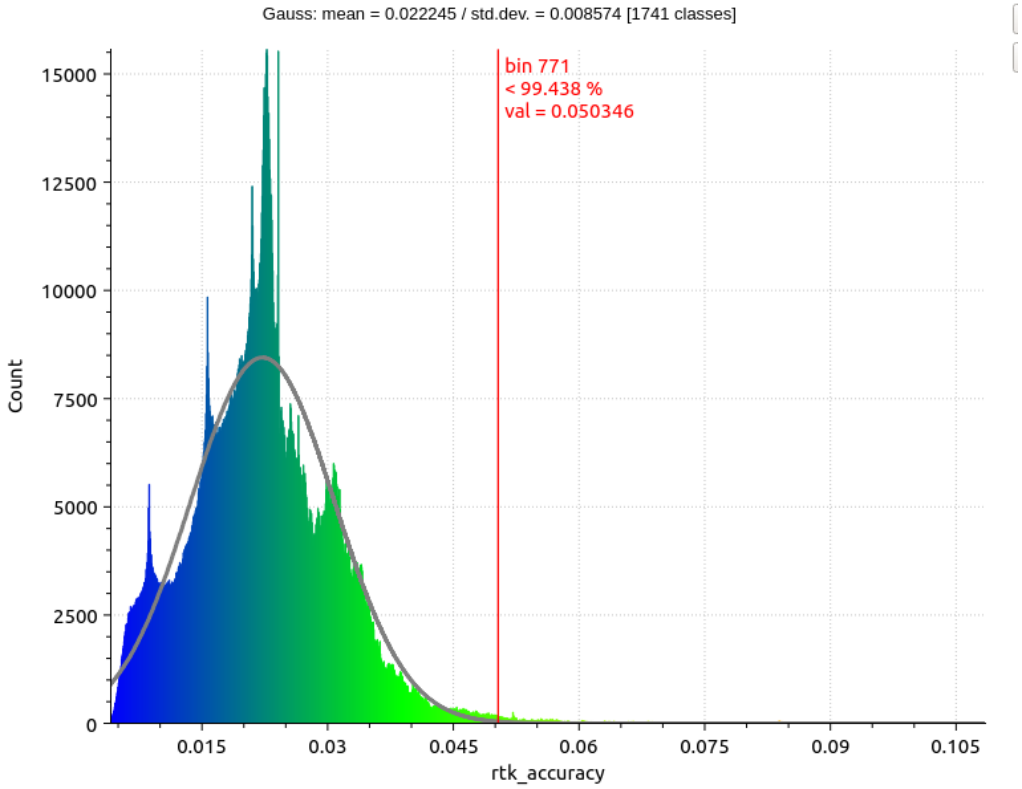

Figure 10 The mean error distribution associated with the observed global RTK accuracy

A closer look at the heat map under the flight trajectory is provided in **Figure 11**. It can be seen that blue regions are formed mainly under the flight trajectory. However, with a higher concentration on the regions, that flight path has more intersections and overlaps such as the area indicated by a yellow rectangle compared to areas with no trajectory overlaps such as the area indicated by a pink rectangle.

The reason for such a phenomenon is the reinforcing effect of RTK observations that occurs when multiple observations are applied to the same region of the point cloud. This is because the points in that region have several RTK observations associated with them, which increases their accuracy. This can be compared to the presence of a GCP (Ground Control Point) target, which enhances the accuracy of a point cloud when it is observed. However, as the point cloud moves away from that observed point, its accuracy may decline as it becomes increasingly reliant on SLAM alone.

To maximize high-accuracy regions (blue regions in **Figure 9**), plan the flight trajectory to include more self-intersections. This is because RTK observations increase accuracy with more self-intersections.

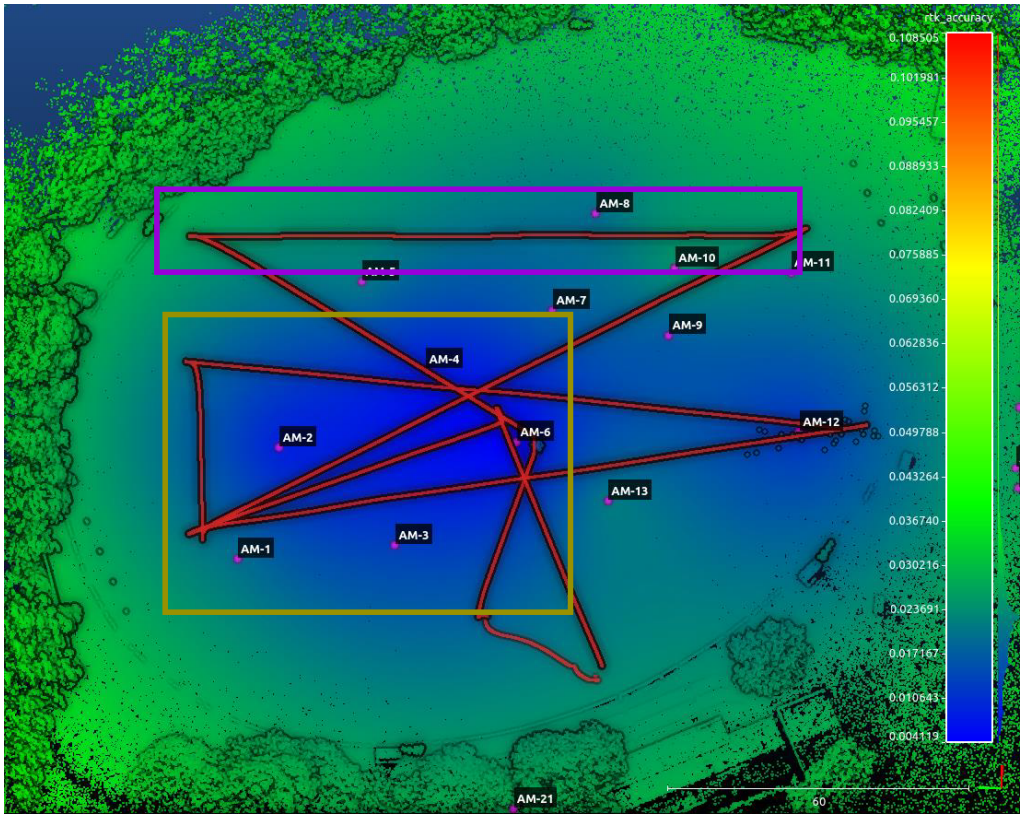

Figure 11 Reinforcing effect of overlapped flight paths in forming high accuracy (blue) regions

In addition to blue regions, we can observe the formation of green regions as the distance of points to the trajectory (where RTK constraints are made) is increased. It can be seen how the range of the LiDAR return to the trajectory affects the resulting “global” RTK accuracy in that location (i.e. there is an inverse relationship between range and accuracy).

For example, as illustrated in **Figure 12**, the horizontal accuracy at target “AM-25” is approximately 50mm at ~102m from the trajectory, compared to ~11mm which was observed at target “AM-12” which is 30m from the trajectory.

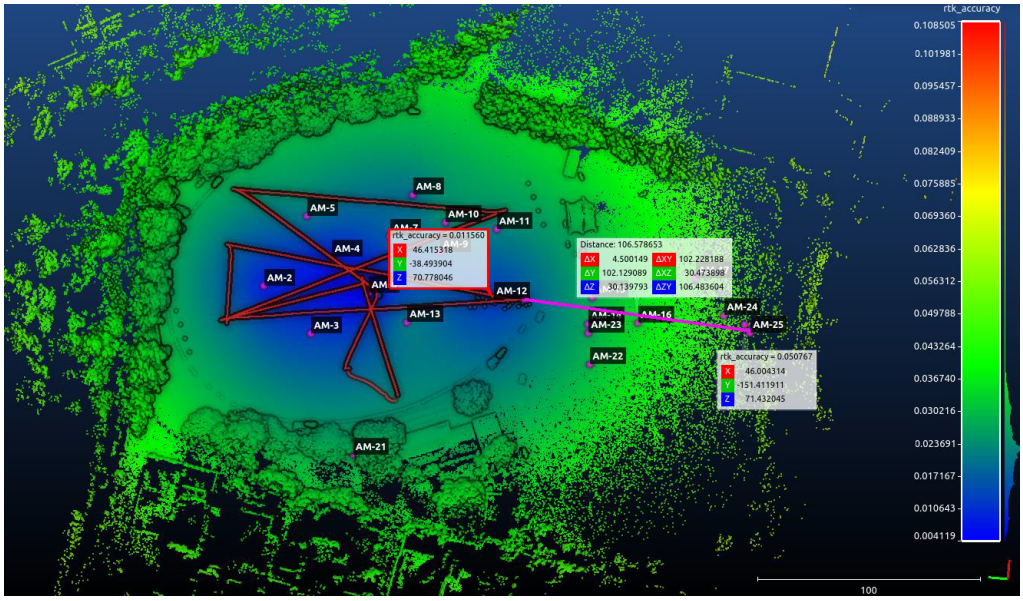

Figure 12 Distance measures illustrating the effect of distance (range) on LiDAR return accuracy relative to their proximity to the scan trajectory

5.1 RTK Accuracy at Different Ranges

After analyzing the global accuracy observed (focused at a 30m range from the trajectory) in **Figure 13**, it was found that the central area has a greenish color, indicating an error of less than 24.5mm. Additionally, some blue areas with greater accuracy were observed due to the RTK constraints overlap. However, as the trajectory moves away from the central area, yellow and red regions start appearing. **Figure 14** shows that these bands of yellow and red are within two and three standard deviations of the error distribution.

Based on the standard deviation of 4.6 mm, the accuracy at the red band starts at about three standard deviations away from the mean error distribution. This means that the error should be 13.8mm more than the mean error value. From a distance measurement, it was found that the distance between the inner edge of low-accuracy regions (red regions) to the closest RTK observation (trajectory point) is around 30 meters. Therefore, it can be said that the geo-referencing error at 30m away from the nearest RTK constraint point (pink dashed arc in Figure 13) will settle at about μ+3s (as they belong to orange and red regions), which is 23.4 + 3 x 4.6 = 37.2mm.

As per this analysis, it is recommended that parallel flight trajectories should not be planned more than 30 meters away from each other to maintain accuracy within an acceptable range.

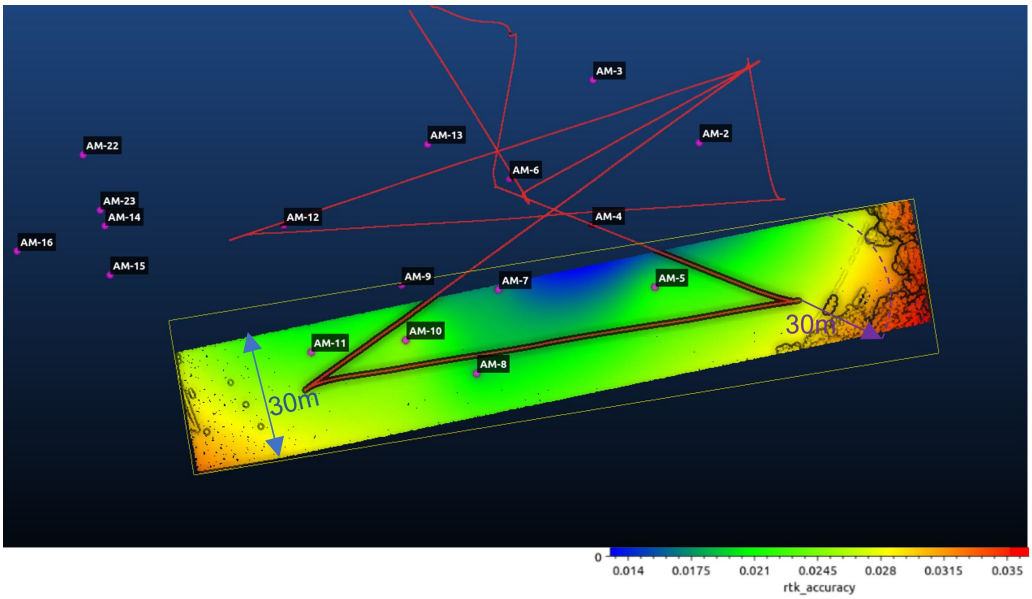

Figure 13 **Error heatmap for a 30m wide band corresponding to a straight flight path**

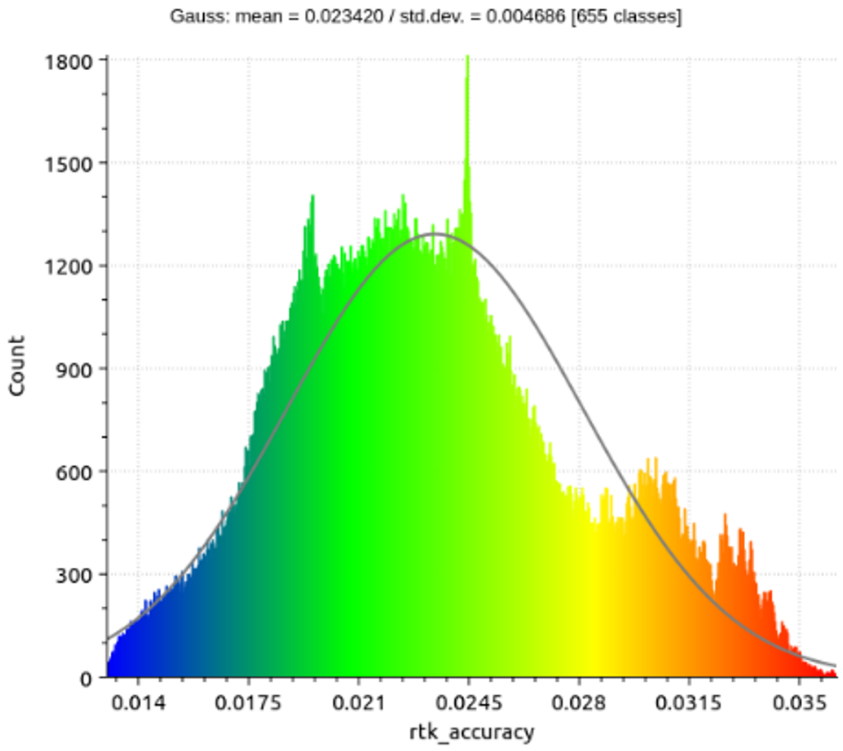

Figure 14 **Error histogram corresponding to the band on Figure 10**

6. Conclusion

This article explained how RTK data can be used to improve the accuracy of the Emesent SLAM algorithm and avoid drift and slips while delivering accurate georeferenced point clouds. An overview of the processing pipeline was presented and provided insights into the system internals to help manage end-user expectations covering the evaluation steps of the system, experiment setup, and analysis of results.

The georeferencing error statistics were analyzed, and the results indicated that horizontal accuracy for the M300 falls within 20mm±12mm, vertical accuracy is within 38mm±6mm, and 45mm±8mm can be achieved for 3D accuracy. For M350, horizontal accuracy falls within 18mm±9mm, vertical accuracy is within 22mm±15mm, and 30mm±15mm for 3D accuracy. Our extensive analysis also showed that 50mm accuracy on the M300 and M350 RTK can be achieved with 90% confidence.

The concept of implicit georeferencing and how the flight trajectory can affect the accuracy of the point cloud were discussed. Based on analysis, overlaps in flight trajectory can enhance accuracy, particularly in situations where the RTK standard deviation is large. However, these results are based on a limited number of experiments, and the accuracy of the system may vary based on RTK quality, environment structure, flight path, velocity, altitude, and other parameters.

Overall, these findings are for indication purposes only, and the performance of the system should be evaluated based on the specific circumstances in which it is used.

We are continually evaluating the system's performance under various conditions, and we will publish the results of these evaluations.

emesent

PREPARED BY:
EMESENT PTY LTD
LEVEL G, BUILDING 4, KINGS ROW OFFICE PARK
40-52 MCDOUGALL ST, MILTON, QLD, 4064 AUSTRALIA

EMAIL: CUSTOMER-SUCCESS@EMESENT.IO
PHONE: +61 7 3548 9494